Chimeric antigen receptor (CAR) T cell therapy for atherosclerosis

Yuan Liu[1,2], Peizhe Wang[2], Xiaoting Meng[3], Li Kong[2], Keke Fu[3], Xi Kang[4], Yu-Hsuan Tsai[3]*, Joe Z. Zhang[2]*

[1]College of Biological Sciences, China Agricultural University, Beijing, 100193, China

[2]Institute of Neurological and Psychiatric Disorders, Shenzhen Bay Laboratory, Shenzhen, 518132, China

[3]Institute of Molecular Physiology, Shenzhen Bay Laboratory, Shenzhen, 518132, China

[4]Translational Innovation Center, Shenzhen Bay Laboratory, Shenzhen, 518132, China

*Email: tsai.y-h@outlook.com; joezhang@szbl.ac.cn

Dear Editor,

Atherosclerosis is a chronic disease of the arterial wall initiated by excessive accumulation of low-density lipoprotein (LDL) particles in the arterial intima. Oxidized LDL is taken up by macrophages, driving their transformation into foamy macrophages (also known as foam cells), a hallmark of atherosclerotic plaques.[1] foamy macrophages are a major component of fatty streaks and actively promote disease progression by sustaining inflammation, enhancing lipid accumulation, and disrupting local tissue homeostasis.[2] Over time, these cells undergo diverse forms of programmed cell death, thereby contributing to the formation and expansion of necrotic cores and reducing plaque stability.[3] Despite their central roles in both initiation and progression of atherosclerosis, precision therapeutics specifically targeting foamy macrophages are not yet available. Instead, current preventive strategies rely largely on systemic risk-factor control, particularly lipid lowering. Although cholesterol-lowering therapies have slowed atherosclerosis progression, substantial residual cardiovascular risk persists even in individuals with well-controlled circulating cholesterol levels, underscoring the need for new targeted therapeutic paradigms.[4]

Recent advances in cellular immunotherapy directed against cell-surface antigens have shown remarkable efficacy in multiple cancers.[5] More recently, this approach has been extended beyond oncology. Chimeric antigen receptor (CAR) T cells targeting cardiac fibroblasts in cardiac fibrosis,[6,7] senescent cells in aging,[8,9] and B cells in autoimmune disease,[10] have demonstrated therapeutic potential through selective depletion of disease-driving cell populations. Given the pathogenic role of foamy macrophages in atherosclerosis, we hypothesized that selectively eliminating these cells using a CAR T cell approach could confer anti-atherosclerotic benefit.

To identify a suitable cell-surface marker enriched in foamy macrophages, we integrated multiple publicly available single-cell RNA-sequencing (scRNA-seq) datasets from human arteries and mouse

aortas. Macrophages constituted one of the major cellular components in these datasets (**Fig. S1**). Subclustering of the macrophages revealed multiple subpopulations, consistent with the current view of macrophage heterogeneity,[11] with foamy macrophages representing the predominant subset in both human and mouse arteries (**Figs. 1a-b** and **S1**). Among genes highly expressed in foamy macrophages, TREM2 emerged as one of the top three cell-surface markers in both species (**Fig. 1c-e**), consistent with recent studies.[12,13] Together, these findings identify TREM2 as a promising candidate for targeting foamy macrophages.

As epitope choice can substantially shape CAR T cell activity, we explored TREM2 targeting using multiple binding modules. We specifically selected three distinct single-chain variable fragments (scFvs) from independent sources, each previously reported to recognize both human and mouse TREM2. This cross-species reactivity was central to our study design, as atherosclerosis is best modelled in immunocompetent mice, whereas the immunodeficient strains commonly used for CAR T cell studies have impaired macrophage biology. Cross-species recognition may also facilitate future translational development.

To generate TREM2-targeting CARs, we selected three distinct single-chain variable fragments (scFvs) and, for each, constructed both human and mouse CARs containing the corresponding human or mouse CD28 and CD3ζ intracellular domains. This yielded six CAR constructs in total: hCAR1-3 and mCAR1-3 (**Fig. S2a-b**). The human constructs were introduced into primary human T cells by lentiviral transduction to generate hCAR1-3 T cells, while the mouse constructs were introduced into primary mouse T cells by retroviral transduction to generate mCAR1-3 T cells. Primary T cells were activated for 48 h before viral transduction, yielding more than 60% CAR positive cells by day 4 (**Fig. 1f**). We first evaluated human CAR T cells against human target cells. When co-cultured with Trem2-positive THP1, all three types of CAR T cells exhibited potent cytotoxicity, whereas cytotoxicity against Trem2-negative

NALM6 cells was negligible, indicating Trem2-dependent target-cell killing (**Figs. 1g** and **S2c**). Mouse CAR T cells were then evaluated against mouse target cells. mCAR1-3 T cells efficiently killed TREM2-positive RAW264.7 cells, but showed minimal activity against TREM2-negative MC38 cells (**Figs. 1h** and **S2d**). Target cell lysis was accompanied by IFNγ and TNFα secretion, with hCAR1 and mCAR1-2 T cells eliciting the strongest cytokine responses (**Fig. 1i** and **j**).

Because the activity of human CAR T cells could not be readily assessed *in vivo* in murine models of atherosclerosis, we established a vessel organoid (VO) system to evaluate target-cell killing in a more tissue-relevant setting. we established a co-culture system consisting of human induced pluripotent stem cell-derived VOs, THP1 cells, and human CAR T cells (**Fig. 1k**). In this model, CAR T cells efficiently eliminated THP1 cells without detectable disruption of vascular integrity, as assessed by vessel area and total junction number (**Fig. 1l-n**).

Given the robust activity observed *in vitro*, we next evaluated the *in vivo* therapeutic efficacy using the *Apoe*$^{-/-}$ model of atherosclerosis. After 12 weeks of high-fat diet (HFD) feeding, mice received 5×10^6 mouse CAR T cells by tail-vein injection, and aortas were analyzed 4 weeks later. En face Oil Red O (ORO) staining showed that mCAR1 significantly reduced plaque area by approximately 30%, whereas mCAR2 and mCAR3 produced more modest effects (**Fig. 1o**). This reduction was particularly evident in the descending aorta (**Fig. S3a)**. Consistently, analysis of aortic root sections confirmed that mCAR1 T cells significantly decreased plaque burden (**Figs. 1p** and **S3b-c**). In addition, mCAR1 and mCAR3 significantly reduced necrotic core area (**Fig. 1q**). Plaque reduction was accompanied by decreased infiltration of CD68+ macrophages, and the abundance of Trem2+ macrophages was also markedly reduced in the mCAR1-treated group (**Fig. 1r**).

Notably, the therapeutic effects of CAR T cells were independent of systemic lipid metabolism, as serum LDL-C, total cholesterol (TC), and triglyceride (TG) levels did not differ between treated and untreated mice (**Fig. S4a-c**), indicating that plaque reduction was not attributable to altered circulating lipid levels. In addition, serum IFNγ and TNFα levels at 3 and 7 days after treatment were comparable across groups (**Fig. S4d-e**), indicating there was no overt cytokine storm. We also did not observe obvious organ toxicity as determined by the histological analysis (**Fig. S5**).

Because mCAR1 T cells showed the strongest therapeutic efficacy in *Apoe*$^{-/-}$ mice, we further evaluated this construct in two additional models of atherosclerosis: *Ldlr*$^{-/-}$ mice and AAV8-PCSK9-treated mice. In both models, mice were fed a HFD for 16 weeks before the treatment, and aortas were analyzed 4 weeks later. En face ORO staining revealed that mCAR1 T cells significantly reduced total plaque area in both models by approximately 50% in *Ldlr*$^{-/-}$ mice and 30% in the AAV8-PCSK9 model (**Figs. 1s-t** and **S6a-b**). Consistent with the findings in *Apoe*$^{-/-}$ mice, analysis of aortic root sections showed reductions in plaque size, necrotic core area, and Trem2+ macrophage content within lesions (**Figs. 1u-y** and **S6c-d**).

In summary, our study provides proof of concept that selective depletion of TREM2+ foamy macrophages reduces plaque burden and necrotic core size across three preclinical models of atherosclerosis without affecting circulating lipid levels. Recent demonstration of the efficacy of anti-oxLDL CAR Treg therapy in atherosclerosis further highlights the promise of cellular immunotherapy for this disease.[14] Although TREM2 has a well-established role in macrophage lipid uptake, prior studies manipulating TREM2 in macrophages have yielded divergent effects on atherosclerotic plaque development. [12,13,15] In contrast, we targeted TREM2+ macrophages for depletion rather than attempting to modulate TREM2 signaling, and observed robust therapeutic benefit. Collectively, these findings establish foamy macrophages as an actionable target and provide a framework for the development of

immunotherapies for atherosclerosis. Future studies should address the dependence of efficacy on epitope specificity, as well as the biodistribution and persistence of CAR T cells.

References

1. Libby, P. *Nature* **592**, 524-533 (2021).
2. Moore, K.J., Sheedy, F.J., and Fisher, E.A. *Nat Rev Immunol* **13**, 709-721 (2013).
3. De Meyer et al. *Nat Rev Cardiol* **21**, 321-325 (2024).
4. Tan, S.H et al. *World J Cardiol* **18**, 114960 (2026).
5. Zugasti, I et al. *Signal Transduct Target Ther* **10**, 210 (2025).
6. Aghajanian, H et al. *Nature* **573**, 430-433 (2019).
7. Rurik, J.G et al. *Science* **375**, 91-96 (2022).
8. Amor, C et al. *Nature* **583**, 127-132 (2020).
9. Yang, D et al. *Sci Transl Med* **15**, eadd1951 (2023).
10. Schett, G., Mackensen, A., and Mougiakakos, D. *Lancet* **402**, 2034-2044 (2023).
11. Murray, P.J., and Wynn, T.A. *Nat Rev Immunol* **11**, 723-737 (2011).
12. Patterson, M.T et al. *Nat Cardiovasc Res* **2**, 1015-1031 (2023).
13. Piollet, M et al. *Nat Cardiovasc Res* **3**, 269-282 (2024).
14. Schwab, R.D et al. *Circulation* **153**, 319-337. (2025).
15. Guo, X et al. *Cell. Mol. Life Sci.* **80**, 137. (2023).

Acknowledgements

We thank SZBL, National Natural Science Foundation of China (82370311 and W2432052) and the Shenzhen Medical Research Fund (D2501002) for financial support, Mr Shoujin Jiang for conducting preliminary experiments for this project, and the SZBL Biomedical Research Core Facilities and Laboratory Animal Center for technical assistance.

Author Contributions

YL, XM, LK, KF: conducted the *in vitro* experiments and analyzed the data. YL: conducted the *in vivo* experiments and analyzed the data. PW: analyzed the scRNA-seq data. YL, XK, YHT, and JZZ: wrote and edited the manuscript. YHT and JZZ: conceived the idea and provided funding support.

Conflict of Interest

The authors declare no competing interests.

Figure Legend

Chimeric antigen receptor (CAR) T cell therapy for atherosclerosis. **a-b.** UMAP visualization of monocyte/macrophage subpopulations identified by integration of scRNA-seq datasets from human arteries and mouse aortas. **c-d.** Heat maps showing genes upregulated in foamy macrophage clusters relative to the other six human monocyte/macrophage clusters (**c**) or the other nine mouse clusters (**d**). **e.** Top three significantly enriched cell-surface marker genes in foamy macrophages. **f.** flow cytometric analysis of the expression of CARs in human (left) and mouse (right) primary T cells 4 days after transduction. **g-h.** TREM2-dependent *in vitro* cytotoxicity of human (**g**) and mouse (**h**) CAR T cells. Human CAR T cells were co-cultured with NALM6 or THP1 cells at an effector : target (E:T) ratio of 1:20 for 4 days; mouse CAR T cells were co-cultured with MC38 or RAW264.7 cells at an E:T ratio of 1:10 for 4 days. $n = 3$ independent experiments. **i-j.** IFN-γ and TNF-α levels in human(**i**) and mouse (**j**) co-culture supernatants measured by ELISA. $n = 3$ independent experiments. **k.** Representative immunofluorescence images of hiPSC-derived blood vessel organoids stained for CD31 and Hoechst 33342, showing CD31+ vascular structures. Organoids were co-cultured with THP1 cells and human CAR T cells for 4 days. **l.** Cytotoxicity of three human CAR T-cell products against THP1 cells in the blood vessel organoid co-culture system. $n = 4$ organoids per group. **m-n.** Quantification of vessel area (**m**) and total junction number (**n**) in blood vessel organoids using AngioTool. $n = 4$ organoids per group. **o.** En face Oil Red O (ORO) staining of whole aortas and quantification of plaque area in *Apoe-/-* mice. $n = 10$ mice per group. **p.** ORO staining of aortic roots and quantification of plaque area. $n = 10$ mice per group. **q.** Masson's trichrome staining of aortic roots and quantification of necrotic core area. $n = 5$ mice per group. **r.** Immunofluorescence staining of aortic roots for CD68+ and Trem2+, with quantification of CD68+ and Trem2+ areas. $n = 7$ mice per group. **s-t.** En face ORO staining of whole aortas and quantification of plaque area in *Ldlr-/-* mice (**s**) and AAV8-PCSK9-treated mice (**t**). $n = 5$ mice per group. **u.** ORO staining of aortic roots and quantification of plaque area in *Ldlr-/-* mice and AAV8-PCSK9-treated mice. $n = 5$ mice per group. **v.** Masson's trichrome staining of aortic roots and quantification of necrotic core area in *Ldlr-/-* mice and AAV8-PCSK9-treated mice. $n = 5$ mice per group. **w.** Immunofluorescence staining of aortic roots for CD68 and Trem2. **x-y.** quantification of CD68+ (**x**) and Trem2+ (**y**) areas in *Ldlr-/-* mice and AAV8-PCSK9-treated mice. $n = 5$ mice per group. $^{*}P < 0.05$, $^{**}P < 0.01$, $^{***}P < 0.001$, $^{****}P < 0.0001$. Scale bars, 200 μm; bottom images in **r** and **w**, 50 μm.

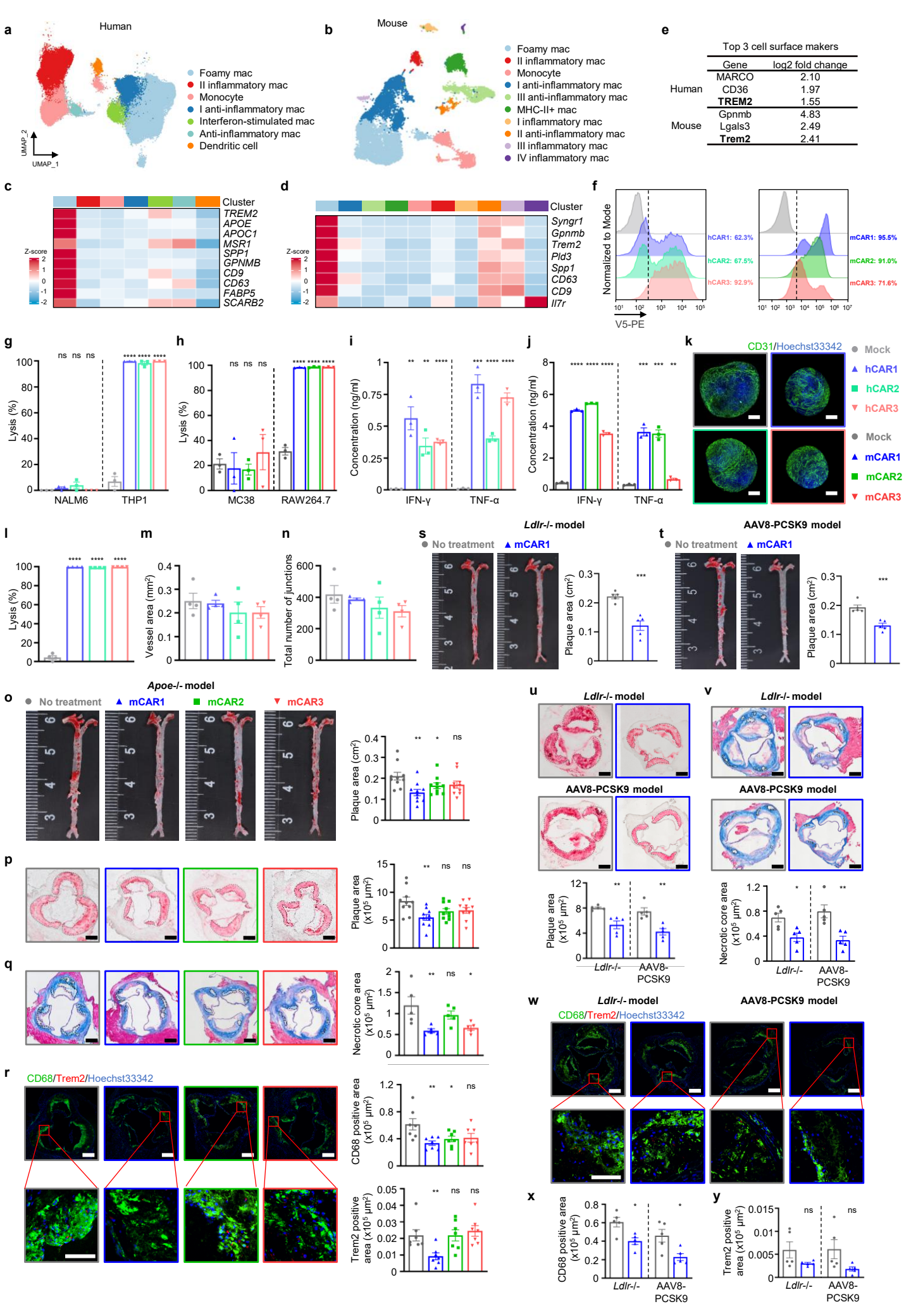
a
Human
Foamy mac
II inflammatory mac
Monocyte
I anti-inflammatory mac
Interferon-stimulated mac
Anti-inflammatory mac
Dendritic cell
UMAP_2
UMAP_1
b
Mouse
Foamy mac
II inflammatory mac
Monocyte
I anti-inflammatory mac
III anti-inflammatory mac
MHC-II+ mac
I inflammatory mac
II anti-inflammatory mac
III inflammatory mac
IV inflammatory mac
e
Top 3 cell surface makers
Gene
log2 fold change
Human
MARCO 2.10
CD36 1.97
TREM2 1.55
Mouse
Gpnmb 4.83
Lgals3 2.49
Trem2 2.41
c
Cluster
TREM2
APOE
APOC1
MSR1
SPP1
GPNMB
CD9
CD63
FABP5
SCARB2
Z-score
d
Cluster
Syngr1
Gpnmb
Trem2
Pld3
Spp1
CD63
CD9
Il7r
Z-score
f
Normalized to Mode
hCAR1: 62.3%
hCAR2: 67.5%
hCAR3: 92.9%
mCAR1: 95.5%
mCAR2: 91.0%
mCAR3: 71.6%
V5-PE
g
Lysis (%)
NALM6
THP1
h
Lysis (%)
MC38
RAW264.7
i
Concentration (ng/ml)
IFN-γ
TNF-α
j
Concentration (ng/ml)
IFN-γ
TNF-α
k
CD31/Hoechst33342
Mock
hCAR1
hCAR2
hCAR3
Mock
mCAR1
mCAR2
mCAR3
l
Lysis (%)
m
Vessel area (mm²)
n
Total number of junctions
s
Ldlr-/- model
No treatment
mCAR1
Plaque area (cm²)
t
AAV8-PCSK9 model
No treatment
mCAR1
Plaque area (cm²)
o
Apoe-/- model
No treatment
mCAR1
mCAR2
mCAR3
Plaque area (cm²)
p
Plaque area (x10⁵ μm²)
q
Necrotic core area (x10⁵ μm²)
r
CD68/Trem2/Hoechst33342
CD68 positive area (x10⁵ μm²)
Trem2 positive area (x10⁵ μm²)
u
Ldlr-/- model
AAV8-PCSK9 model
Plaque area (x10⁵ μm²)
Ldlr-/-
AAV8-PCSK9
v
Ldlr-/- model
AAV8-PCSK9 model
Necrotic core area (x10⁵ μm²)
Ldlr-/-
AAV8-PCSK9
w
Ldlr-/- model
AAV8-PCSK9 model
CD68/Trem2/Hoechst33342
x
CD68 positive area (x10⁵ μm²)
Ldlr-/-
AAV8-PCSK9
y
Trem2 positive area (x10⁵ μm²)
Ldlr-/-
AAV8-PCSK9